Nuclear Materials and Energy 16 (2018) 88–94

Contents lists available at ScienceDirect

Nuclear Materials and Energy

journal homepage: www.elsevier.com/locate/nme

Improvement of EUROFER's mechanical properties by optimized chemical compositions and thermo-mechanical treatments

J. Hoffmann*, M. Rieth, M. Klimenkov, S. Baumgärtner

Karlsruhe Institute of Technology, Karlsruhe 76021, Germany

A B S T R A C T

9%Cr reduced activation steels are the designated structural materials for future fusion reactors. The improvement of this class of alloys, especially for the extension of the operation limits, is the present scope of the EUROfusion materials project for advanced steels. Within this programme, new alloys are designed and fabricated to overcome some of the limitations of EUROFER97.

In the present study, four 9%Cr alloys with some variations in the chemical compositions are compared to standard EUROFER97 batches. The main focus lies in the possible extension of the operation window to both higher and lower temperatures. The limits of the mechanical properties, which can be achieved through different heat and thermo-mechanical treatments, are explored within this work. The thermo-mechanical treatments used within this work consist of rolling within the austenite regime and rapid (water-) quenching to room temperature. Toughness from Charpy impact tests, creep to rupture lifetime and tensile strength are compared for the different treatments. EBSD and STEM investigations of the formed microstructures complete the presented work.

Strong effects of the heat-treatments on the toughness and strength were observed. As expected, hardening the materials beyond the conventional treatment (980 °C/30 min + 750 °C/2 h) showed a major increase in tensile strength and decrease in toughness. Moderate variations in the alloy compositions open the possibility for extended temperature windows for these unconventional heat treatments (e.g. higher tempering temperature). Thermo-mechanical treatments are effective to improve hardening and other properties by modifications of the distribution of secondary phases. As expected, the different heat treatments also showed the well-known effects on the mechanical properties (e.g. hardness and strength). When compared, the effects of heat treatments on the mechanical properties are far beyond the influence of minor changes in the alloy compositions.

1. Introduction

Future fusion reactors demand for structural materials which can withstand high neutron doses and still provide acceptable mechanical properties. A significant part of the EUROfusion materials research programme is dedicated towards the optimization of 9%-Cr EUROFER and variants of its composition.

With multiple blanket concepts which utilize different principles, coolants and operation temperatures, there is a strong demand for an extension of the operation windows 9%-Cr steels [1,2]. This applies to both lower and higher temperature extensions for water-cooled and helium-cooled applications within the first wall.

The work on dedicated alloys for water-cooled applications is focused towards high toughness and low ductile-to-brittle transition temperature (DBTT) values. The regime of the operation temperatures (below 300 °C) combined with an estimated damage of more than 20 dpa causes severe neutron embrittlement within the structural materials [3,4]. The observed shift in DBTT may be compensated with a very low starting DBTT and a larger tolerable deterioration of the properties. $M_{23}C_6$ chromium-rich carbides have a tendency to coarsen and hence reduce the ductility and toughness of the 9%-Cr steels. Reducing the amount of carbon in the alloys is an effective method to reduce the precipitation of $M_{23}C_6$ and promote the formation of fine MX carbides and nitrides.

Helium-cooled applications demand for materials with improved high temperature (tensile) strength and prolonged creep to rupture lifetimes. It has already been demonstrated on conventional EUROFER97 and other 9%-Cr steels that ausforming processes within the austenite-regime are effective to gain creep performance [5,6]. Modifications to the alloy compositions can change the secondary phase precipitation and may result in an optimized size distribution of stable carbide and nitrides to provide added high temperature strengthening

* Corresponding author.
E-mail address: j.hoffmann@kit.edu (J. Hoffmann).

https://doi.org/10.1016/j.nme.2018.05.028
Received 14 December 2017; Received in revised form 2 May 2018; Accepted 31 May 2018

[7].

The scope of this work are four new 9%-Cr alloys. These alloys were produced with small variations in the chemical compositions. These materials are then characterized by electron microscopy and mechanical testing such as tensile, Charpy impact and creep tests. The results are compared to EUROFER97 and rated according to the following targets:

- High toughness values on the upper shelf leg and a lower DBTT than EUROFER97 (Charpy impact testing).
- Reduce the amount of $M_{23}C_6$ carbides and increase small and fine dispersed MC carbides or MN nitrides (M = Ta, V).
- Increase high temperature strength (tensile tests).
- Reach creep to rupture lifetimes beyond EUROFER97.

The first target is aimed towards water cooled applications, while the later three are to optimize the materials and the properties for higher operating temperatures.

2. Experimental

Four different alloys were produced at OCAS NV, Zelzate Belgium. They were produced by Vacuum Induction Melting (VIM) with a batch size of approx. 100 kg. The chemical compositions (real composition measured by chemical analysis) are given in Table 1. The compositions varied in terms of the V and Ta content (promote VN, TaC precipitation) as well as the C content (reduce amount of $M_{23}C_6$ precipitation).

A thermo-mechanical treatment concluded the production process. An initial rolling at 1150 °C (roughening) was followed by further rolling and slow cooling down to 900 °C. This processing was performed within the austenite regime (so called ausforming) and should optimize the distribution of the secondary phases such as carbides and nitrides. The materials were water quenched after the last rolling step. This condition will be referred to thermo-mechanically treated (TMT) throughout the text.

Different heat treatments with combinations of austenitization and tempering were applied to the materials to promote either low temperature performance (e.g. DBTT) or increase high temperature properties (e.g. creep). These treatments consist of tempering at 750 °C or 820 °C for 2 h after TMT + WQ. Additional treatments were performed with an austenitization at 950 °C/1000 °C for 30 min followed by tempering between 750 °C and 840 °C (depending on the material). The respective HTs of the materials are given at the corresponding figures. Heat treatment for EUROFER97 was always 980 °C/30 min and 750 °C/2 h.

The time temperature transition diagrams were measured with a Netsch 402ED dilatometer. Cylindrical specimens were measured against a Al_2O_3 reference cylinder in static Helium atmosphere to prevent too much oxidation. Prior to the actual measurement, the materials were heated up to 1000 °C with a heating rate of 5 K/min and held for 1 h with subsequent cooling (5 K/min cooling rate) to 100 °C. This step removed the TMT microstructure through a full austenitization. The experiments from there on were performed with 5 K/min heating to 1000 °C and then cooling with different rates (20 K/min down to 0.8 K/min).

Table 1
chemical compositions of the alloys used in this study. All contents in wt. %. (courtesy of Chemical Analytik, IAM-AWP).

No.	Cr	W	V	Ta	C	N
J361	8.7	1.14	0.2	0.09	0.105	0.05
J362	8.7	1.07	0.35	0.1	0.058	0.05
J363	8.7	1.08	0.35	0.09	0.11	0.05
J364	8.7	0.97	0.29	–	0.059	0.05
EUROFER97	8.9	1.1	0.2	0.14	0.1	0.02

Mechanical tests were performed by using KLST (3 mm × 4 mm × 27 mm, V-notch 60° angle/1 mm depth) Charpy impact specimen, flat tensile specimen (38 mm length, 2 mm × 1 mm gauge and 9.71 gauge length) and cylindrical creep specimen (d = 5 mm, 56 mm length, 25 mm gauge length). Creep tests were performed in air.

A Zeiss Merlin equipped with an EDAX Hikkari high speed EBSD camera was used for the microstructural characterization. The maps were measured at 20 kV with a current of 10 nA. Points with a confidence index (CI) lower than 0.1 were discarded for the maps. Apart from a CI standardization, no cleanup was performed on the EBSD maps. Points exceeding a misorientation of 15° are considered high angle boundaries (marked in black) and those with a misorientation between 5° and 15° are marked in white (sub-grain boundaries). EDX mappings and STEM images were acquired with a FEI Tecnai F20 field emission gun transmission electron microscope operated at 200 kV.

3. Results and discussion

While some materials (J361, J363) were designed with carbon content similar to EUROFER97, it was lowered for J362 and J364. Since carbon is an important factor to form a fully martensitic structure, it has to be checked whether this microstructure can be achieved with reasonable and technically feasible cooling speeds. Fig. 1 shows the measured time temperature transition (TTT-) diagrams for two alloys with the different levels of carbon (0.1 and 0.06%). The critical cooling rate increased from 4 K/min to more than 20 K/min. However, these rates can still be achieved by cooling the materials in air and ensures a fully martensitic structure even for larger components.

TMT produces a non-typical microstructure for 9%-Cr steels with elongated prior austenite grains (PAG) along the rolling direction. This is shown in the EBSD maps in Fig. 2 for two alloys with different carbon contents. The microstructure consists of fully tempered martensite, but is rather inhomogeneous and contains a high degree of deformation and dislocation substructure within the martensite packets. This has already been confirmed by previous works and analyzed by transmission electron microscopy [5].

After a complete heat treatment consisting of austenitization, quenching and tempering (A + Q + T), the materials will form a homogeneous microstructure with smaller and equiaxed PAGs and a less pronounced sub-structure within the packets and laths. This is shown in Fig. 3.

EDX mappings of the materials J361 and J362 proved that the reduction in carbon is effective to reduce the amount of coarse chromium-rich $M_{23}C_6$ carbide (compositions see Table 2). These particles are marked with red circles (Figs. 4 and 5) and are present in the Cr, Ta and V maps. The compositions of the $M_{23}C_6$ particles are similar to compositions reported for EUROFER97 by Klimenkov et al. and Stratil et al. [8,9]. Due to the influence of the surrounding matrix, the carbon or nitrogen content of the particles cannot be measured precisely. The increase in V and N content of J362 and J363 promoted the formation of vanadium-rich precipitates. These are presumably vanadium nitrides [8]. However, these small secondary phases showed a tendency to agglomerate instead of forming a fine dispersed distribution. The material J361 showed a similar size distribution of the precipitates like EUROFER97 [5,10].

The size distributions of the secondary phases in alloys J361 and J363 were measured on TEM extraction replica with EDS mappings and are shown in Fig. 6. The alloy modification with an increased V content in J363 promotes the formation of V-rich precipitates. The size distribution of the Ta-rich precipitates showed only minor differences. The additional amount of carbon and nitrogen which could be bound due to increased V levels did not affect the Ta(C,N) precipitation.

The TMT, which was applied to the materials, was aimed towards high temperature performance. Unfortunately, this leads to a shift in DBTT towards higher temperatures. Even a very high tempering

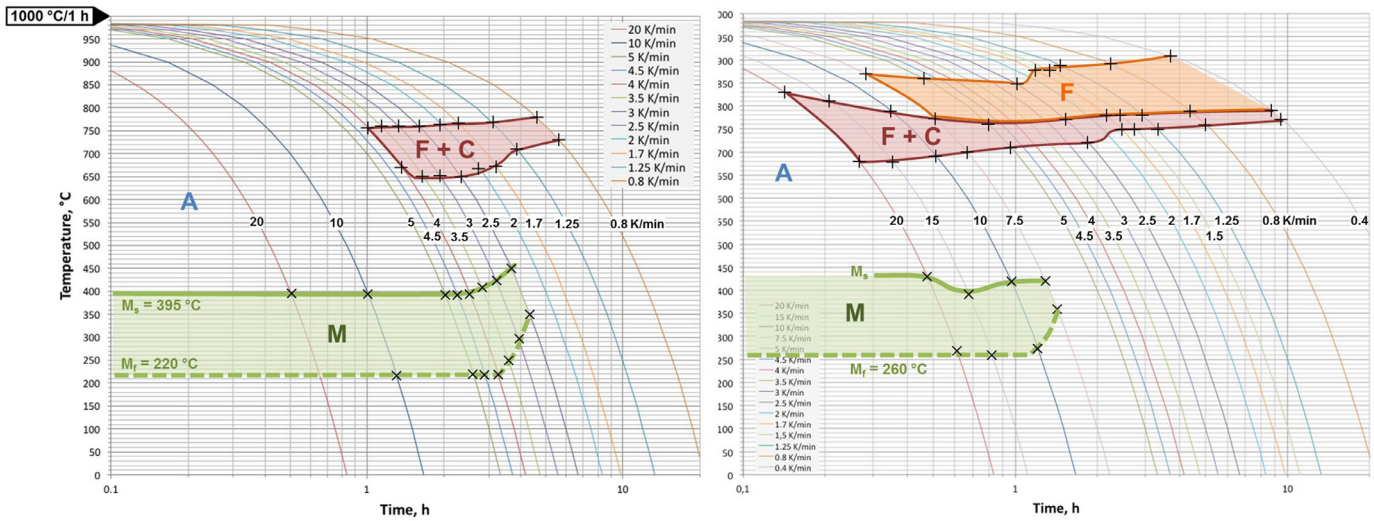

Fig. 1. time temperature transition diagram of J361 (left) and J362 (right) showing the effect of carbon content on the critical cooling speed for martensite transformation. The different occurring phases are marked with letters (A: austenite, F: ferrite, C: carbide, M: martensite).

temperature of 820 °C (Fig. 7a)) is not able to compensate this shift. Interestingly, the upper shelf energy (USE) remains almost unchanged and is within the range of EUROFER97 in standard conditions [11]. If optimized heat treatments resulting from the TTT diagrams are performed, the DBTT of the materials can be improved up to the performance of EUROFER97 and beyond. The diagram can be used to find the right temperatures for the heat treatments to result in a fine and homogeneous microstructure (in the quenched and tempered state). An example is given for the alloy J362 in Fig. 7b) where its DBTT reached similar temperatures compared to the reference EUROFER97. The USE reached even higher values of up to 12.5 J.

The tensile properties of the materials after various treatments are shown in Fig. 8. Fig. 8a) shows the beneficial effect of the TMT for materials J361 and J362. With no tantalum and a vanadium content of only 0.29%, material J364 lacks strength compared to the others. Even TMT could not increase the strength over the reference material EUROFER97 (with no TMT added). With no improved properties in terms of DBTT, toughness and strength, J364 clearly shows no benefits over EUROFER97. Studies by Wakai et al. also looked into the effect of different heat treatments on the Charpy impact properties [12]. They reported increased DBTT values due to inhomogeneities in the distribution of the secondary phases rising from repeated heat treatments. Similar Inhomogeneities were caused by the TMT to the materials in the present study which caused the observed DBTT shifts. Additionally, Stratil et al. [9] also found that an increased sub-structure size (e.g. PAG size) is detrimental for both toughness and transition temperature.

The large range of adjustable strength of the materials is shown in Fig. 8b). A very good performance in Charpy impact tests comes with the drawback of very low strength in tensile tests. However, austenitization at 1000 °C and tempering at 820 °C of J361 still showed high temperature yield strength above 600 °C which was comparable to the TMT + tempered materials.

Creep tests reveal the real benefits of TMT treatments in this study. In Fig. 9, a Larson-Miller-plot of all performed creep tests is shown. Material J361 reached nearly the same performance as conventional EUROER97 when normalized at 1000 °C and tempered at 750 °C. However, when TMT was applied, the creep strength increased significantly with a nearly 50 °C gain in operation temperature or an order of magnitude increased creep to rupture lifetime. This effect is strongly correlated on the elongated microstructure which results from the TMT treatments. Similar results have been obtained in earlier studies for

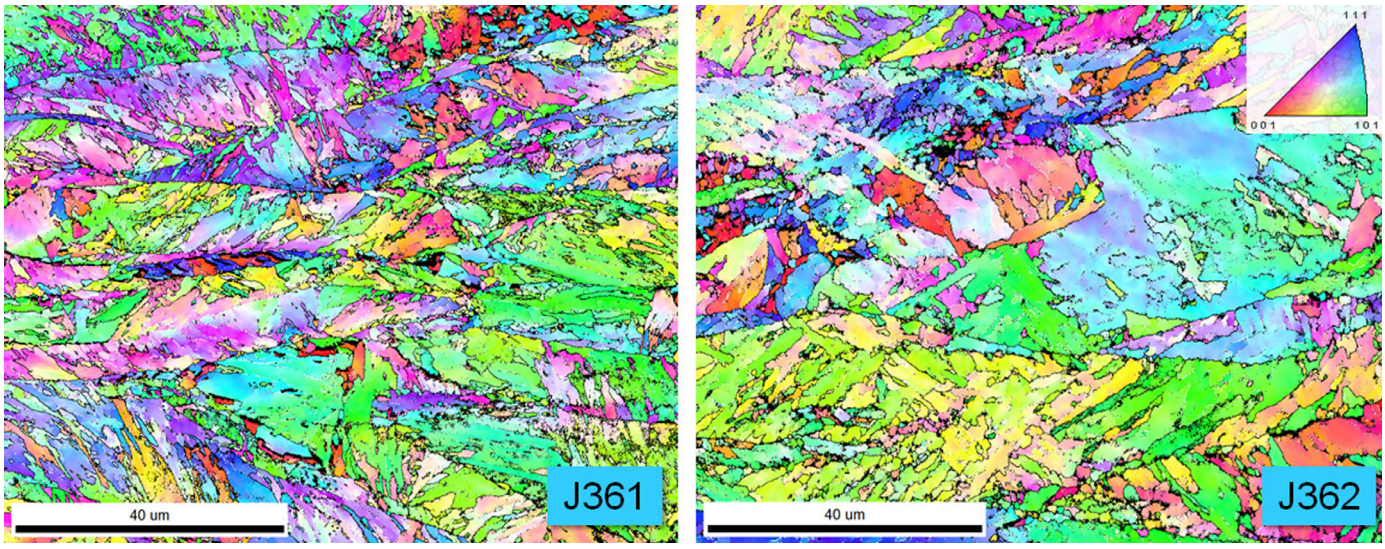

Fig. 2. EBSD maps of J361 and J362 after thermo-mechanical treatment, water quenching and tempering at 750 °C for 2 h.

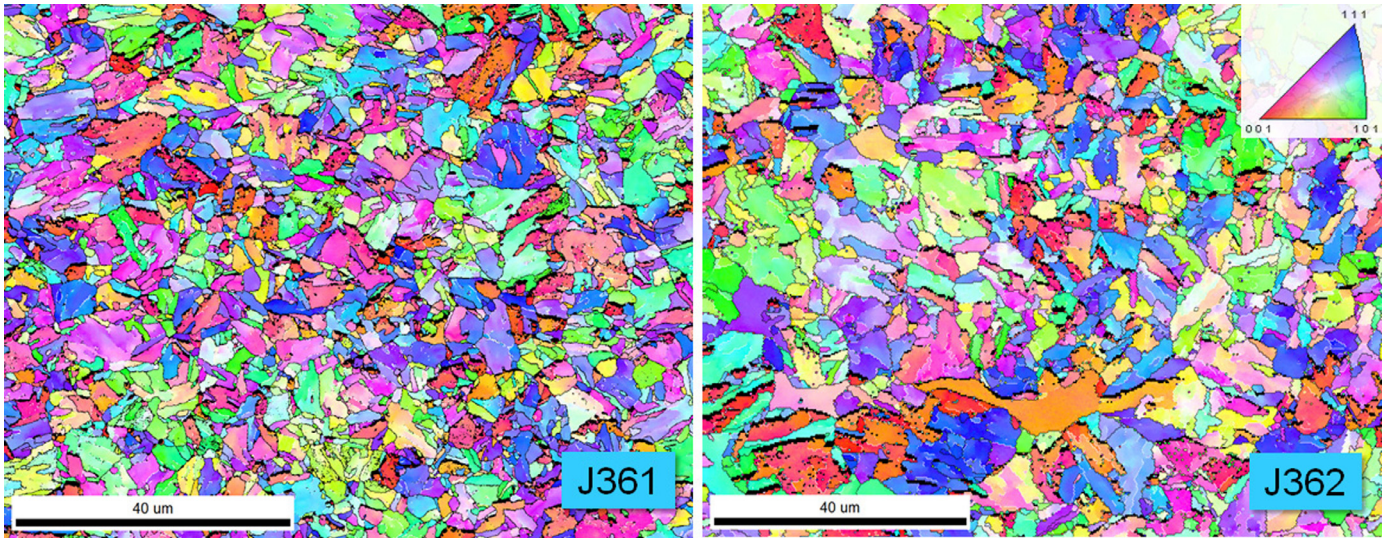

Fig. 3. EBSD maps of J361 and J362 after full heat treatment consisting of normalizing at 1150 °C for 30 min, water quenching and tempering at 750 °C for 2 h.

Table 2
Compositions of M23C6 secondary phases after tempering at 825 °C (J361 and J363) and 750 °C (EUROFER97).

Alloy	Fe	Cr	W	V	Ta
J361	30.87 ± 1.41	64.77 ± 1.42	3.69 ± 0.41	0.60 ± 0.30	0.40 ± 0.00
J363	32.20 ± 2.20	62.32 ± 2.32	23.00 ± 3.00	1.83 ± .83	0.50 ± .50
EUROFER97 [9]	26 ± 2	61 ± 2	9 ± 1	Minor amount	Minor amount

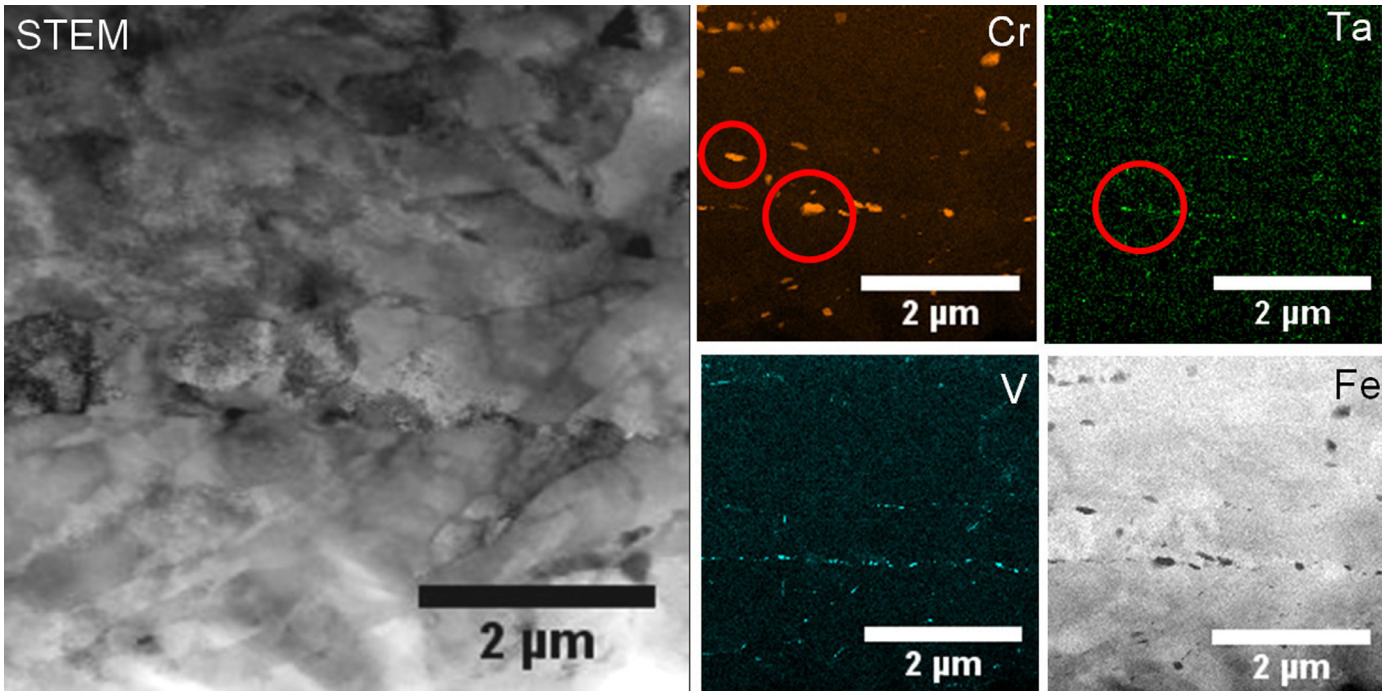

Fig. 4. TEM analysis of the precipitate structure after TMT + 750 °C/2 h (Material J361). STEM image shown in inverse contrast.

EUROFER heat-treated the same way [5]. This effect may be not as prominent if the materials are not tested with specimens taken out in rolling direction.

4. Conclusions

Four different 9%-Cr steels were produced with small variations in the chemical composition and compared against EUOFER97. The following effects were observed:

(1) The chemical variations of the materials gave rise to different heat treatments of the materials. This has been demonstrated by the TTT diagrams. The carbon content has the strongest effect on the formation of the different phases. Especially, the critical cooling speed to form a fully martensitic structure needs to be taken care of to remain within reasonable technical limits.

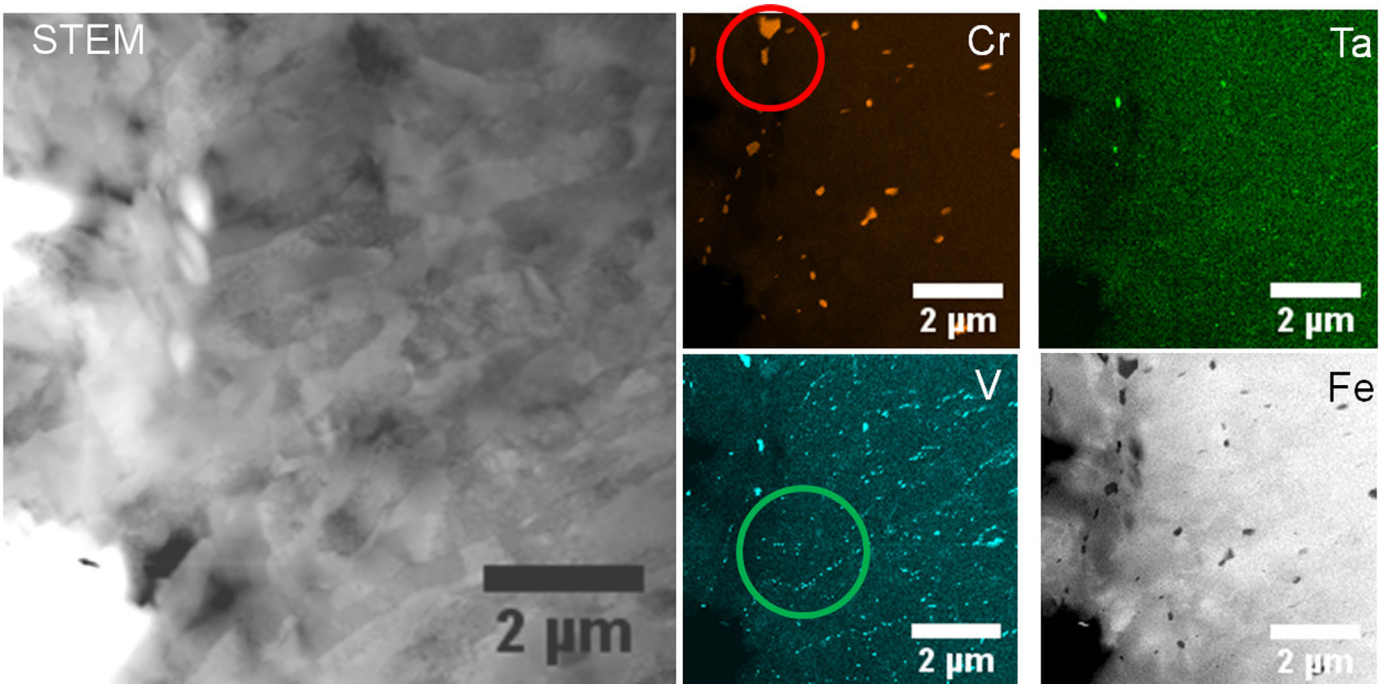

Fig. 5. TEM analysis of the precipitate structure after TMT + 750 °C/2 h (Material J362). STEM image shown in inverse contrast.

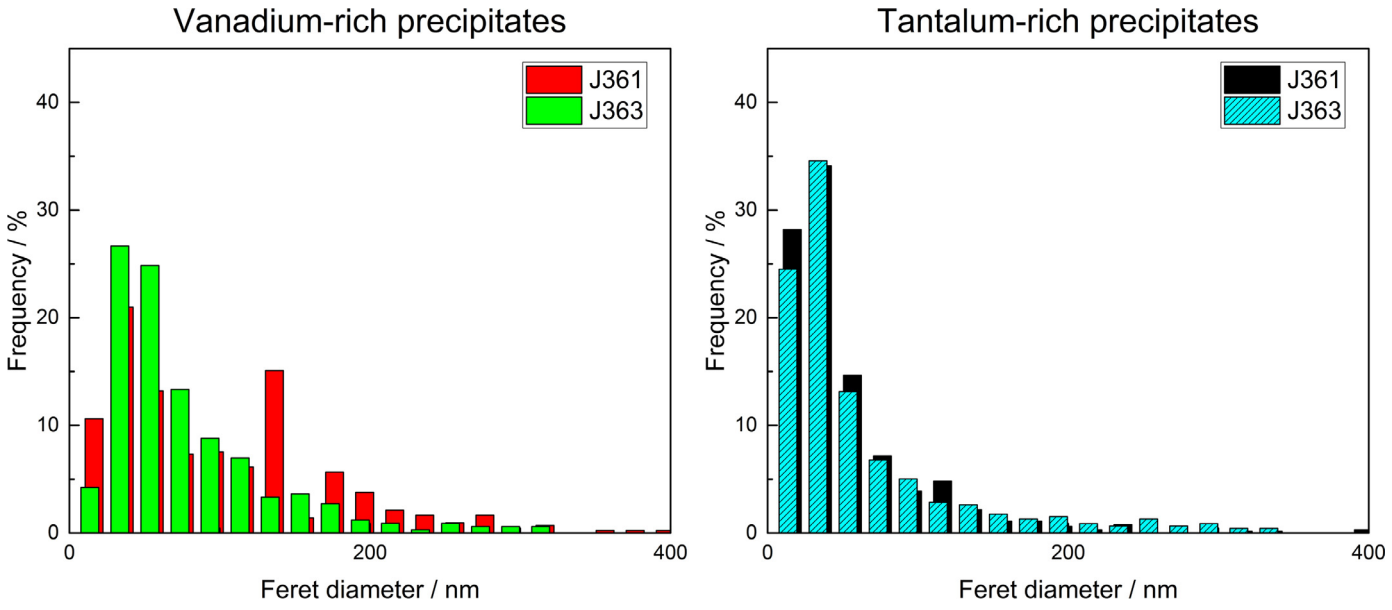

Fig. 6. Size distribution of the secondary phases containing V and Ta for alloys J361 and J363.

(2) The microstructure after ausforming was elongated in the direction of the rolling and showed high degrees of dislocations with a pronounced sub-structure within the PAGs and packets. An austenitization and tempering treatment formed a well-known tempered martensitic microstructure with small PAGs and defined packets and laths. The secondary phases forming independently of the heat treatments were carbo-nitrides rich in chromium, tantalum (not in J364) and vanadium.

(3) The thermo-mechanical treatments proved to detrimental for the toughness (e.g. upper shelf energy) and DBTT of the materials. However, removing the treatments and performing a full normalizing and tempering treatment increased the properties to the desired level. Material J362 with lower carbon content even surpassed EUROFER with a slightly lower DBTT and 1.5 J increase in USE. The increased sub structure size (e.g. PAG size) and inhomogeneities within the distribution of secondary phases are responsible for the lower DBTT and USE values.

(4) TMT treatments showed improvements in terms of high temperature strength for most materials. An exception was material J364 (without Ta addition) were no clear effect of the rolling was

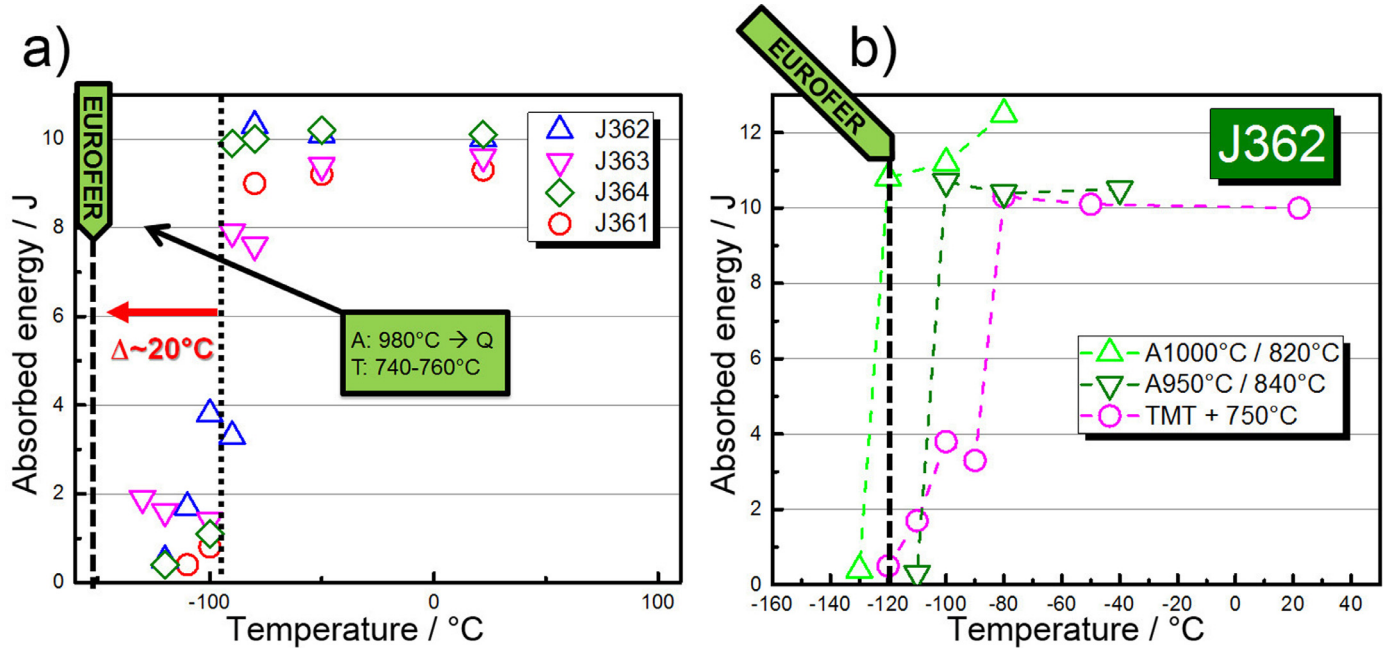

Fig. 7. Charpy impact tests of the different materials. Materials after TMT + 820 °C/h tempering compared to EUROFER97 in 980 °C/740 °C condition (non-TMT) (a)). Material J362 with "removed" TMT compared and different A + Q + T to EUROFER97 in 980 °C/740 °C condition (b)).

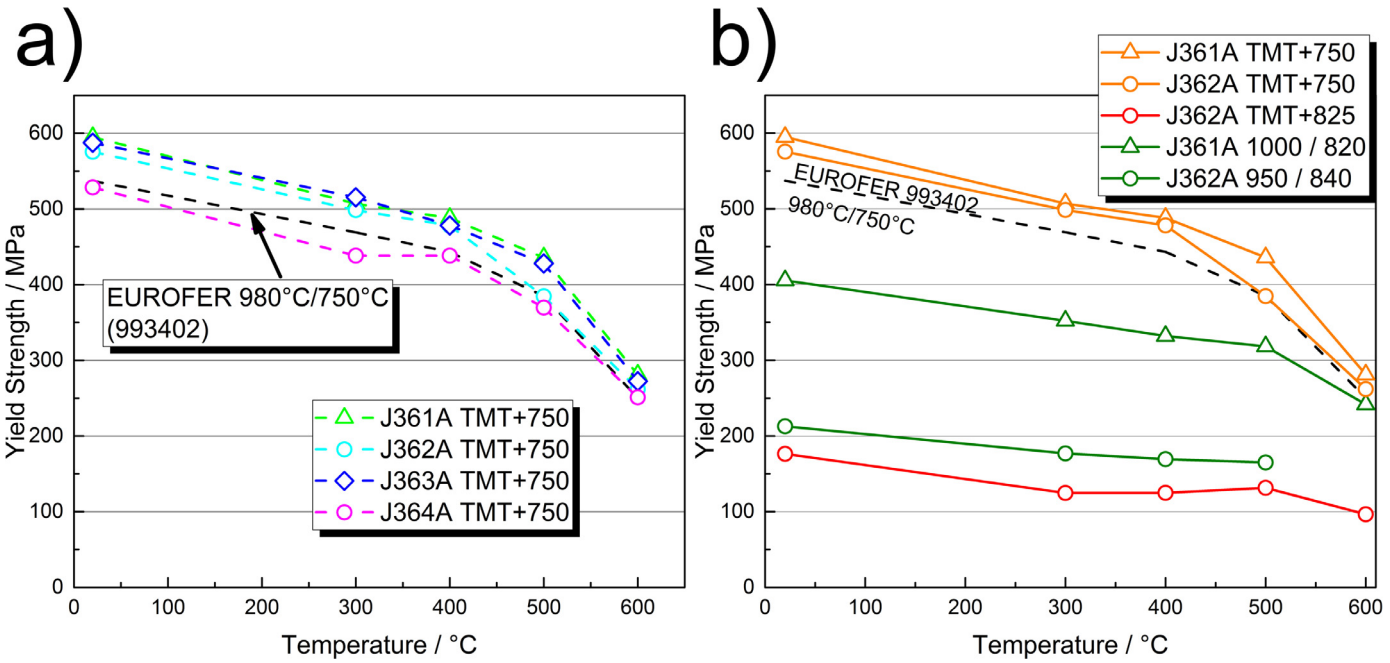

Fig. 8. tensile tests of the materials. (a) Effect of TMT treatment of the different materials compared to EUROFER97. (b) Strength of materials J361 and J362 after different thermal treatments.

observed and the properties remained below EUROFER97. Creep performance had a very clear benefit from the TMT with J361 extending the creep to rupture time by an order of magnitude or increasing the possible operation temperature by nearly 50 °C. Improvements were also found for alloy J632 and J363. Previous studies have also shown that TMT is effective to improve materials with standard EUROFER97 compositions [5]. Creep strength of the materials in the tested temperature regime is dominated by dislocation movement (glide and climb) [13]. Combined with the microstructure which is elongated towards the tensile load, the

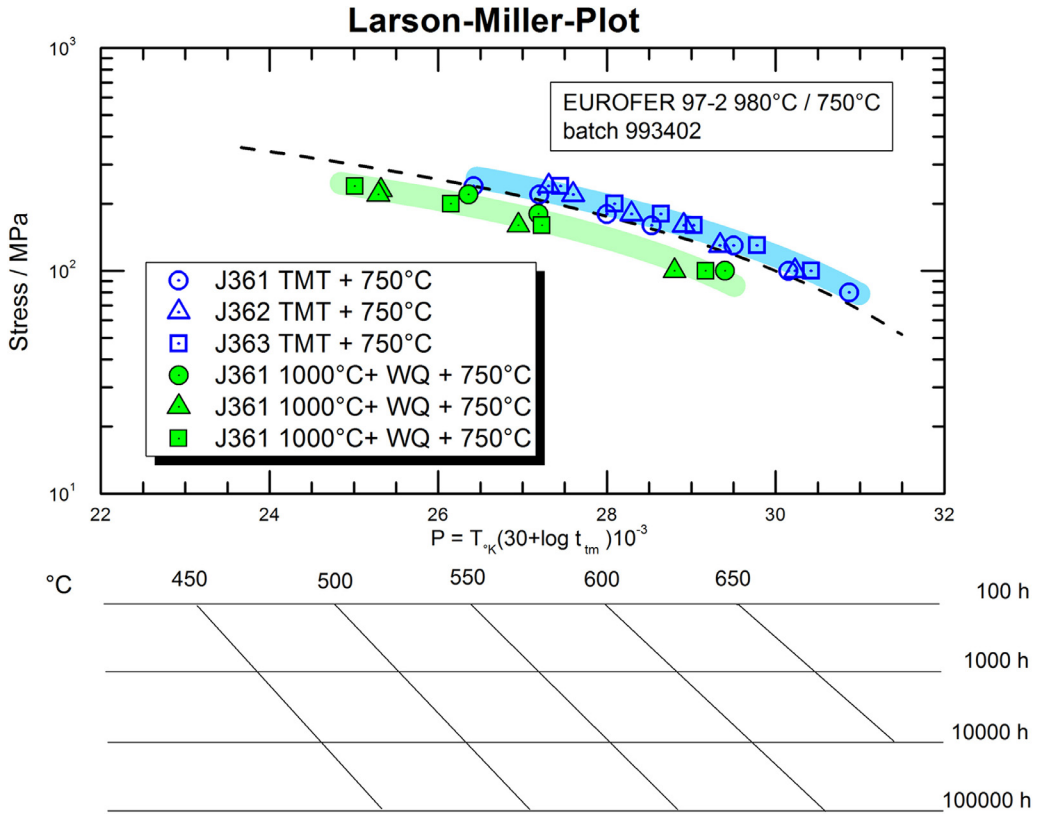

Fig. 9. Larson–Miller-Plot of the creep experiments with different loads and temperature on TMT and non-TMT materials. The dashed line represents EUROFER97/2.

increased amount of finer particles present after TMT is also effective to increase creep strength.

Acknowledgments

This work has been carried out within the framework of the EUROfusion Consortium and has received funding from the Euratom research and training programme 2014-2018 under grant agreement No 633053. The views and opinions expressed herein do not necessarily reflect those of the European Commission.

D. Bolich, S. Heger, M. Hoffmann, J. Jung, K. Kaleta, S. Sickinger and the department for chemical analysis (IAM-AWP CA) are acknowledged for the mechanical, microstructural and chemical characterizations.

Supplementary materials

Supplementary material associated with this article can be found, in the online version, at doi:10.1016/j.nme.2018.05.028.

References

[1] M. Enoeda, H. Tanigawa, T. Hirose, S. Suzuki, K. Ochiai, C. Konno, Y. Kawamura, T. Yamanishi, T. Hoshino, M. Nakamichi, H. Tanigawa, K. Ezato, Y. Seki, A. Yoshikawa, D. Tsuru, M. Akiba, Fusion Eng. Des. 87 (2012) 1363–1369.
[2] J.F. Salavy, G. Aiello, P. Aubert, L.V. Boccaccini, M. Daichendt, G. De Dinechin, E. Diegele, L.M. Giancarli, R. Lässer, H. Neuberger, Y. Poitevin, Y. Stephan, G. Rampal, E. Rigal, J. Nucl. Mater. 386–388 (2009) 922–926.
[3] M. Kytka, M. Brumovsky, M. Falcnik, J. Nucl. Mater. 409 (2011) 147–152.
[4] E. Gaganidze, H.C. Schneider, B. Dafferner, J. Aktaa, J. Nucl. Mater. 367–370 A (2007) 81–85.
[5] J. Hoffmann, M. Rieth, L. Commin, P. Fernández, M. Roldán, Nucl. Mater. Energy 6 (2016) 12–17.
[6] R.L. Klueh, N. Hashimoto, P.J. Maziasz, J. Nucl. Mater. 367–370 (2007) 48–53.
[7] L. Tan, L.L. Snead, Y. Katoh, J. Nucl. Mater. 478 (2016) 42–49.
[8] M. Klimenkov, R. Lindau, E. Materna-Morris, A. Möslang, Prog. Nucl. Energy 57 (2012) 8–13.
[9] L. Stratil, H. Hadraba, J. Bursik, I. Dlouhy, J. Nucl. Mater. 416 (2011) 311–317.
[10] P. Fernández, A.M. Lancha, J. Lapeña, M. Serrano, M. Hernández-Mayoral, J. Nucl. Mater. 307–311 (2002) 495–499.
[11] H. Tanigawa, E. Gaganidze, T. Hirose, M. Ando, S.J. Zinkle, R. Lindau, E. Diegele, Nucl. Fusion 57 (2017) 92004.
[12] E. Wakai, M. Ando, N. Okubo, J. Plasma Fusion Res. 11 (2015) 104–112.
[13] G. Yu, N. Nita, N. Baluc, Fusion Eng. Des. 75–79 (2005) 1037–1041.